

Improved Patch-Clamp Techniques for High-Resolution Current Recording from Cells and Cell-Free Membrane Patches

O. P. Hamill, A. Marty, E. Neher, B. Sakmann, and F. J. Sigworth

Max-Planck-Institut für biophysikalische Chemie, Postfach 968, Am Fassberg, D-3400 Göttingen, Federal Republic of Germany

Abstract. 1. The extracellular patch clamp method, which first allowed the detection of single channel currents in biological membranes, has been further refined to enable higher current resolution, direct membrane patch potential control, and physical isolation of membrane patches.

2. A description of a convenient method for the fabrication of patch recording pipettes is given together with procedures followed to achieve giga-seals i.e. pipette-membrane seals with resistances of 10^9 – 10^{11} Ω .

3. The basic patch clamp recording circuit, and designs for improved frequency response are described along with the present limitations in recording the currents from single channels.

4. Procedures for preparation and recording from three representative cell types are given. Some properties of single acetylcholine-activated channels in muscle membrane are described to illustrate the improved current and time resolution achieved with giga-seals.

5. A description is given of the various ways that patches of membrane can be physically isolated from cells. This isolation enables the recording of single channel currents with well-defined solutions on both sides of the membrane. Two types of isolated cell-free patch configurations can be formed: an inside-out patch with its cytoplasmic membrane face exposed to the bath solution, and an outside-out patch with its extracellular membrane face exposed to the bath solution.

6. The application of the method for the recording of ionic currents and internal dialysis of small cells is considered. Single channel resolution can be achieved when recording from whole cells, if the cell diameter is small (< 20 μm).

7. The wide range of cell types amenable to giga-seal formation is discussed.

Key words: Voltage-clamp – Membrane currents – Single channel recording – Ionic channels

Introduction

The extracellular patch clamp technique has allowed, for the first time, the currents in single ionic channels to be observed (Neher and Sakmann 1976). In this technique a small heat-polished glass pipette is pressed against the cell membrane, forming an electrical seal with a resistance of the order of 50 M Ω (Neher et al. 1978). The high resistance of this seal ensures that most of the currents originating in a small patch

of membrane flow into the pipette, and from there into current-measurement circuitry. The resistance of the seal is important also because it determines the level of background noise in the recordings.

Recently it was observed that tight pipette-membrane seals, with resistances of 10–100 G Ω , can be obtained when precautions are taken to keep the pipette surface clean, and when suction is applied to the pipette interior (Neher 1981). We will call these seals “giga-seals” to distinguish them from the conventional, megaohm seals. The high resistance of a “giga-seal” reduces the background noise of the recording by an order of magnitude, and allows a patch of membrane to be voltage-clamped without the use of microelectrodes (Sigworth and Neher 1980).

Giga-seals are also mechanically stable. Following withdrawal from the cell membrane a membrane vesicle forms occluding the pipette tip (Hamill and Sakmann 1981; Neher 1981). The vesicle can be partly disrupted without destroying the giga-seal, leaving a cell-free membrane patch that spans the opening of the pipette tip. This allows single channel current recordings from isolated membrane patches in defined media, as well as solution changes during the measurements (Horn and Patlak 1980; Hamill and Sakmann 1981). Alternatively, after giga-seal formation, the membrane patch can be disrupted keeping the pipette cell-attached. This provides a direct low resistance access to the cell interior which allows potential recording and voltage clamping of small cells.

These improvements of the patch clamp technique make it applicable to a wide variety of electrophysiological problems. We have obtained giga-seals on nearly every cell type we have tried. It should be noted, however, that enzymatic treatment of the cell surface is required in many cases, either as part of the plating procedure for cultured cells, or as part of the preparation of single cells from adult tissues.

In this paper we describe the special equipment, the fabrication of pipettes, and the various cell-attached and cell-free recording configurations we have used. To illustrate the capabilities of the techniques we show recordings of AChR-channel currents in frog muscle fibres and rat myoballs, as well as Na currents and ACh-induced currents in bovine chromaffin cells.

Part I

Techniques and Preparation

Giga-seals are obtained most easily if particular types of pipettes are used and if certain measures of cleanliness are

Send offprint requests to B. Sakmann at the above address

taken. The improved resolution requires a more careful design of the electronic apparatus for lowest possible background noise. These experimental details will be described in this section.

1. Pipette Fabrication and Mechanical Setup

Pipette Fabrication. Patch pipettes are made in a three-stage process: pulling a pipette, coating of its shank with Sylgard, and the final heat polishing of the pipette tip.

First step-pulling: Patch pipettes can be pulled from flint glass or borosilicate glass. Flint glass has a lower melting point, is easier to handle, and forms more stable seals than borosilicate glass, which however has better electrical properties (see below). We routinely use commercially available flint capillaries made for hemocytometric purposes (Cee-Bee hemostat capillaries), or melting point determination capillaries. The borosilicate (Pyrex) glass is in the form of standard microelectrode capillaries (Jencons, H15/10). The pipettes are pulled in two stages using a vertical microelectrode puller (David Kopf Instruments, Tujunga, CA, USA, Model 700C) and standard Nichrome heating coils supplied with it. In the first (pre-)pull the capillary is thinned over a length of 7–10 mm to obtain a minimum diameter of 200 μm . The capillary is then recentered with respect to the heating coil and in the second pull the thinned part breaks, producing two pipettes. To obtain large numbers of pipettes of similar properties it is advisable to use a fixed pulling length and fixed settings for the two stages. For example with Cee-Bee capillaries and the David Kopf puller we use the following settings. The prepull is made at 19A with a pulling length of 8 mm. The thinned part of the capillary is then recentered by a shift of approximately 5.5 mm. The final pull is made at a critical heat setting around 12A. Slight variations of the heat setting around this value produce tip openings between fractions of a μm and several μm . We aim at openings between 1 and 2 μm . These pipettes, then, have steep tapers at the very tip (see for example Fig. 10C). The Pyrex capillaries require higher heat settings of 24 and 15A for the two stages; the resulting pipettes have thicker walls at the tip, and often the tips break unevenly in pulling.

Second step-coating: In order to reduce the pipette-bath capacitance and to form a hydrophobic surface, pipette shanks are coated with Sylgard to within about 50 μm from the tip. Already-mixed Sylgard can be stored for several weeks at -20°C . It is applied to the pipette using a small glass hook taking care that the very tip remains uncoated. We apply the Sylgard while the pipette is mounted in a microforge and cure it by bringing the heated filament close to the pipette for a few seconds. The Sylgard coating is not required for giga-seal formation; it only serves to improve background noise.

Third step — heat polishing: Polishing of the glass wall at the pipette tip is done on a microforge shortly after Sylgard coating. We observe this step at 16×35 magnification using a compound microscope with a long-distance objective. The heat is supplied by a V-shaped platinum-iridium filament bearing a glass ball of ≈ 0.5 mm diameter. The filament is heated to a dull red glow and a stream of air is directed towards the glass ball, restricting the heat to its immediate vicinity. The tip of the pipette is brought to within 10–20 μm of the ball for a few seconds; darkening of the tip walls indicates polishing of the tip rim. If the pipettes are coated with Sylgard, it is preferable to heat-polish them within an

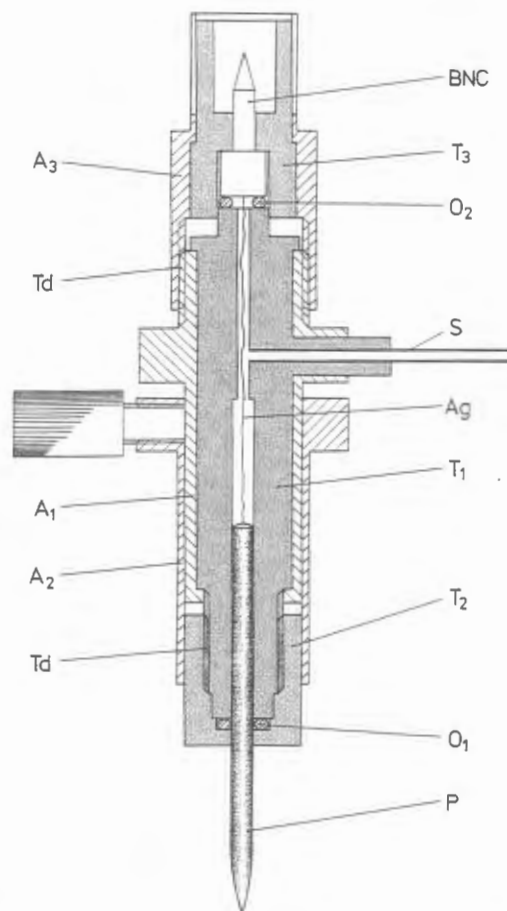


Fig. 1. Cross section through suction pipette holder. The holder serves two basic functions, firstly to provide electrical connection between the patch pipette solution and the pin of a BNC connector, and secondly to allow suction or pressure to be applied to the pipette interior. The holder has a Teflon body T_1 with a central bore for tight fitting of a patch pipette P and a chlorided silver wire Ag which is soldered to the pin of a BNC connector. The BNC pin is held by Teflon piece T_3 . The pipette is tightened by a screw cap T_2 . Outlet S connects to Silicone rubber tubing for application of suction or pressure to the inner compartment, which is made airtight by the O-rings O_1 and O_2 . A_1 and A_3 are aluminium shields to the body; A_2 is a sliding shield to the pipette. Td indicates screw threads. The unit (without pipette) is 55 mm long

hour after coating; after this time, it is difficult to obtain a steep taper at the pipette tip. When pipettes have to be stored more than a few hours they should be cleaned before use by immersion in methanol while a positive pressure is applied to their interior.

Sylgard-coated patch pipettes usually do not fill by capillary forces when their tip is immersed into solution. They can be filled quickly by first sucking in a small amount of pipette solution and then back-filling. All the solutions used for filling should be filtered using effective pore sizes smaller than 0.5 μm . We use pipettes with resistance values in the range 2–5 $\text{M}\Omega$. These have opening diameters between 0.5 and 1 μm .

Mechanical Setup. The patch pipettes are mounted on a suction pipette holder shown schematically in Fig. 1. It consists of inner parts made of Dynal or Teflon T_1, T_2, T_3 and is shielded by metal caps (A_1, A_2, A_3). The outlet S is connected to silicone rubber tubing through which suction is applied, usually by mouth. It is critical that the O-rings, O_1 and O_2 fit tightly. Otherwise the pipette tip can move slightly

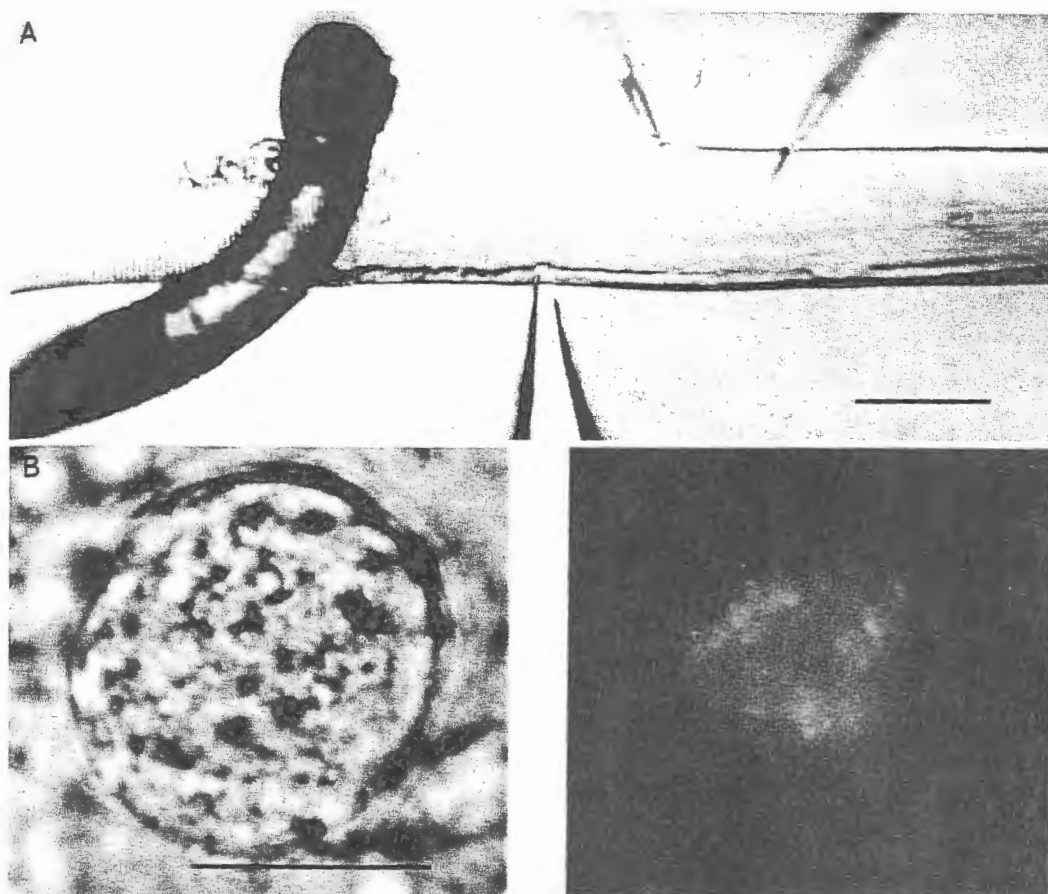


Fig. 2A and B. Single cell preparations used for demonstration of improved patch clamp techniques. (A) Enzyme treated frog (*R. temporaria*) cutaneous pectoris muscle fibre. The end-plate region of this fibre is viewed by Normarski optics. The fibre is supported by a glass hook. The fibre is stripped of its nerve terminal. The patch pipette is seen in contact with the synaptic trough. Two intracellular glass microelectrodes are used here to voltage clamp the fibre locally. Alternatively, the measurement can be performed at the natural resting potential without intracellular electrodes. (B) Primary culture of rat myoball. The same myoball is viewed in bright field optics on the left side and, using fluorescence microscopy, on the right side after labelling with fluorescent Rhodamine-conjugated α -BuTX. The fluorescence pattern illustrates the "patchy"/distribution of AChR's in this preparation. Calibration bars: 50 μ m (upper), and 25 μ m (lower)

during suction, tearing off a membrane patch from the cell. The pipette holder connects to a BNC connector of the amplifier head stage which is mounted on a Narashige MO-103 hydraulic micromanipulator. This, in turn, is mounted onto another manipulator for coarse movements (Narishige MM 33). The pipette holder should be repeatedly cleaned by methanol and a jet of nitrogen.

2. Preparations

The development of giga-seals requires a "clean" plasma membrane; that is, no sign of a surface coat should be detectable in conventionally-stained EM-sections. This requirement is met in many tissue-cultured cells, for example myotubes, spinal cord cells and dorsal root ganglion cells. In adult tissue however individual cells are covered with surface coats and enzymatic cleaning of the cell surface must precede the experiment. The exact protocol of enzymatic cleaning varies from tissue to tissue (see Neher 1981). Here we describe a treatment procedure adequate for frog skeletal muscle fibres. We also briefly describe the preparation of rat myoballs. These cells, as well as the chromaffin cells, require no enzyme treatment before use.

a) End-Plate Region of Frog Muscle Fibres. From innervated muscle a useable preparation can be obtained within 2–3 h

using the following procedure. The whole cutaneous pectoris muscle is bathed for an hour at room temperature in normal frog Ringer solution containing 1 mg/ml collagenase (Sigma type I). At this point overlying fibre layers can be easily cut away, such that a monolayer of fibres remains. The muscle endplate region is subsequently superfused with Ringer solution containing 0.07 mg/ml Protease (Sigma, type VII) for 20–40 min. The tendinous insertions of the muscle fibres are protected by small 3–7 mm guides made from Perspex to restrict the flow of protease containing solution to the endplate region of the muscle (Neher et al. 1978). This procedure results in a preparation of ≈ 20 fibres with ends firmly attached to skin and sternum. When a single fibre is viewed the bare synaptic trough can be easily seen with a $\times 16$ objective (Zeiss 0.32) and $\times 16$ eyepieces using Nomarski interference contrast optics (Fig. 2A). Although currents can be recorded from the synaptic area, the perisynaptic AChR density within 10–50 μ m of the synaptic trough is high enough in most preparations to allow recording of ACh activated single channel currents at low ACh concentrations ($< 1 \mu$ M). Preparations kept in phosphate-buffered Ringer solution remain viable and can be used for up to 48 h when kept at $< 10^\circ$ C. All bath solutions contain 10^{-8} M Tetrodotoxin to avoid muscle contraction during the dissection.

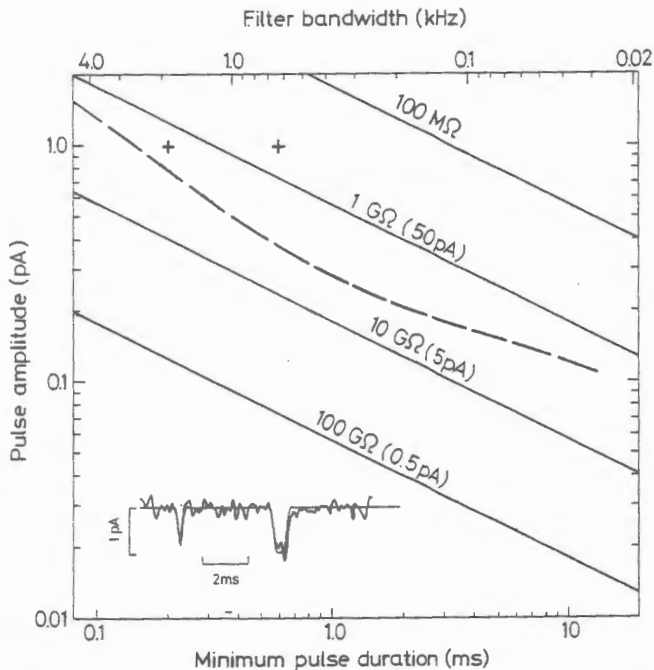


Fig. 3. Limits of pulse detection due to background noise. The relationship between filter settings (top scale) or minimum detectable rectangular pulse durations (bottom scale) and the pulse amplitudes (vertical scale) is shown for various background noise levels. The solid lines represent theoretical limits imposed by Johnson noise and shot noise sources and are discussed below. The dashed curve represents the background noise in an actual recording situation (50 G Ω seal on a myoball) and was computed from the spectrum in Fig. 5. Using this curve and the top scale, an appropriate low-pass filter setting can be found for observing single-channel currents whose amplitude is given by the vertical scale. The filter bandwidths (-3 dB frequency, Gaussian or Bessel response) are chosen to make the standard deviation of the background noise $1/6$ of the given amplitude. When the bottom scale is used the curve shows whether or not a current pulse of given amplitude and duration can be recognized in the presence of the background noise. Each combination of amplitude and duration corresponds to a point in the figure. All points lying above the curve represent pulses that can be detected reliably. For example, 1 pA channel currents can be detected if the duration is at least 0.15 ms; pulses of 0.2 pA amplitude can be detected only if the duration is greater than 2.2 ms. Comparison of the top and bottom scales in the figure then gives the filter setting yielding the best signal-to-noise ratio (peak signal to rms noise) for a pulse of the given minimum duration. However, at this filter setting, the time-course of such a minimum-width pulse is distorted. This is illustrated in the inset, which shows the simulated response of our recording system at 2 kHz to two rectangular pulses, both with original amplitudes of 1 pA but with durations of 0.2 and 0.6 ms. The thin trace shows the response in the absence of noise; in the thicker trace a recording of background noise (same data as in Fig. 5) has been added. The parameters of the two pulses are indicated as crosses in the figure. The shorter pulse represents the movement of 1250 elementary charges; it is clearly detectable, but the *a posteriori*, simultaneous estimation of pulse amplitude and duration is impossible. The rectangular form of the longer pulse is just recognizable, however, allowing these parameters to be estimated. It can be seen from this example that for kinetic analysis of channel gating, the shortest mean event duration should be considerably longer (preferably by an order of magnitude or more) than the minimum given in the figure. The solid lines show the ultimate theoretical detection limits imposed by Johnson noise in the seal and membrane resistance, computed from Eq. (1). Since seal resistances above 100 G Ω are often observed, it should in principle be possible to resolve much smaller pulses than is presently possible. These lines also represent the resolution limits that would be imposed by shot noise (Eq. 2) in channels carrying the indicated current levels in the case that shot noise is the predominant noise source. For the calculation of the detection limits in this figure a filter with Gaussian frequency response was

b) Myoballs from Embryonic Rat Muscle. The procedure to obtain spherical "myoballs" is essentially the same as that used by other laboratories (Horn and Brodwick 1980). The growth medium (DMEM + 10% fetal calf serum) is changed on day 3 and on day 6 after plating of the cells on 18 mm cover slips placed into culture dishes. For 2 days starting on day 8, medium containing 10^{-7} M colchicine is used. Thereafter normal growth medium is used again and changed every third day. This procedure results in ≈ 100 spherical myoballs of 30–80 μ m diameter (Fig. 2B) per cover slip. A single cover slip can be cracked with a scalpel blade into 8–10 small pieces which can be transferred individually into the experimental chamber. The culture medium is exchanged for normal bath solution before the experiment. This solution has the following composition (in mM): 150 NaCl, 3 KCl, 1 MgCl₂, 1 CaCl₂, 10 HEPES, pH adjusted to 7.2 by NaOH.

As visualized with fluorescent α -bungarotoxin, the ACh receptors are unevenly distributed in myoballs (Fig. 2B); however in virtually all patches single channel currents could be recorded with low ACh concentrations ($< 1 \mu$ M). For experiments with ACh-activated channels it is advisable to work within 2–5 days following colchicine treatment. During a later period 5–10 days following colchicine treatment myoballs are a suitable preparation for investigating properties of electrically excitable Na and K channels as well as Ca-dependent K channels.

c) Chromaffin Cells. As an example of cells obtained by enzymatic dispersion of an adult organ we use bovine chromaffin cells. These cells are dispersed by perfusion with collagenase of the adrenal gland (Fenwick et al. 1978), and are subsequently kept in short term culture for up to 8 days (Medium 199, supplemented with 10% fetal calf serum and 1 mg/ml BSA).

3. Background Noise and Design of Recording Electronics

One of the main advantages of the giga-seal recording technique is the improvement, by roughly an order of magnitude, in the resolution of current recordings. The resolution is limited by background noise from the membrane, pipette and recording electronics.

Theoretical Limits. Apart from noise sources in the instrumentation there are inherent limits on the resolution of the patch clamp due to the conductances of the patch membrane and the seal. One noise source is the Johnson noise of the membrane-seal combination, which has a one-sided current spectral density

$$S_I(f) = 4kT \operatorname{Re}\{Y(f)\} \quad (1)$$

where $4kT = 1.6 \times 10^{-20}$ Joule at room temperature, and $\operatorname{Re}\{Y(f)\}$ is the real part of the admittance, which depends, in general, on the frequency f . If the membrane-seal parallel combination is modelled as a simple parallel $R-C$ circuit, then $\operatorname{Re}\{Y(f)\} = 1/R$. Integrating the resulting (in this case constant) spectral density over the frequency range of interest gives the noise variance, which decreases with increasing

assumed; the filter bandwidth was chosen to give a risetime t_r equal to 0.9 times the minimum pulse duration. The minimum detectable pulse amplitude was taken to be 8 times the standard deviation σ of the background noise. A minimum-width pulse is attenuated to 6.7σ by the filter; with a detection threshold of 4.7σ the probability of missing an event is less than 0.02, while the probability per unit time of a background fluctuation being mistaken for a pulse is less than $3 \times 10^{-6}/t_r$.

patch
size of
in Fig.
values

An
expect
through
spectri
cation
made
(Steve

$S_I = 2$

where
assum
unidir
the sa
determ
patch,
in size

Intrin.

backg

times

The e

noise

voltage

Johns

mode

densit

$Re\{Y\}$

where

this

$= (2$

T

thin

unco

when

capac

are i

appa

100 M

high

resist

redu

prev

coati

S

glass

show

capa

close

coat

2 G Ω

least

mor

its h

I

5 M Ω

orde

cons

resu

ble t

patch resistance. From the variance we have calculated the size of the smallest detectable current pulses, which is plotted in Fig. 3 against the minimum pulse durations for various values of R .

Another background noise source is the "shot noise" expected from ions crossing the membrane, for example through leakage channels or pumps. Although the size and spectrum of this noise depends on details in the ion translocation process, a rough estimate of the spectral density can be made assuming that an ion crosses the membrane rapidly (Stevens 1972; Luger 1975),

$$S_j = 2 Iq \quad (2)$$

where q is the effective charge of the current carrier (we assume a unit charge $q_e = 1.6 \times 10^{-19}$ Coulomb) and I is the unidirectional current. The shot noise at $I = 0.5$ pA is nearly the same as the Johnson noise with $R = 100$ G Ω . If R is determined mainly by "leakage channels" in the membrane patch, the shot noise may be comparable to the Johnson noise in size.

Intrinsic Noise in the Pipette. As can be seen in Fig. 3, the background noise in our present recording system is several times larger than the limit imposed by the patch resistance. The excess results from roughly equal contributions from noise sources in the pipette and sources in the current-to-voltage converter. We are aware of three main sources of Johnson noise in the pipette, each of which can be roughly modelled by a series $R-C$ circuit. The current noise spectral density in such a circuit is given by (1) with

$$Re \{ Y(f) \} = \frac{\alpha^2}{R(I + \alpha^2)}, \quad (3)$$

where $\alpha = 2\pi fRC$. In the high frequency limit (α large) this approaches $1/R$; in the low frequency limit $Re \{ Y \} = (2\pi fC)^2 R$, which increases with frequency.

The potentially most serious noise source arises from a thin film of solution that creeps up the outer wall of an uncoated pipette. Evidence for the presence of this film is that, when a small voltage step is applied to the pipette, a slow capacitive transient is observed whose size and time constant are influenced by air currents near the pipette. The film apparently has a distributed resistance R of the order of 100 M Ω , and a distributed wall capacitance $C \approx 3$ pF. In the high frequency regime the noise (like that in a 100 M Ω resistor) is very large. A Sylgard coating applied to the pipette reduces the noise considerably: the hydrophobic surface prevents the formation of a film, and the thickness of the coating reduces C .

Secondly, we find that the bulk conductivity of the pipette glass can be significant. The Cee-Bee capillaries, for example, show substantial conductivity above 100 Hz, as evidenced by capacitance transients and noise spectra from pipettes with closed tips. Coating the pipette helps, but even in a Sylgard-coated pipette the effective values of R and C are roughly 2 G Ω and 2 pF. Pyrex electrode glass (Jencons H15/10) has at least an order of magnitude lower conductivity. However, it is more difficult to make pipettes with this hard glass because of its higher melting point.

Finally, the pipette access resistance R_{acc} (in the range 2–5 M Ω) and the capacitance of the tip of the pipette C_{tip} (of the order of 0.3 pF) constitute a noise source. Since the time constant is short, the low-frequency limit of (3) holds. The resulting spectral density increases as f^2 , becoming comparable to the 1 G Ω noise level around 10 kHz. This noise could be

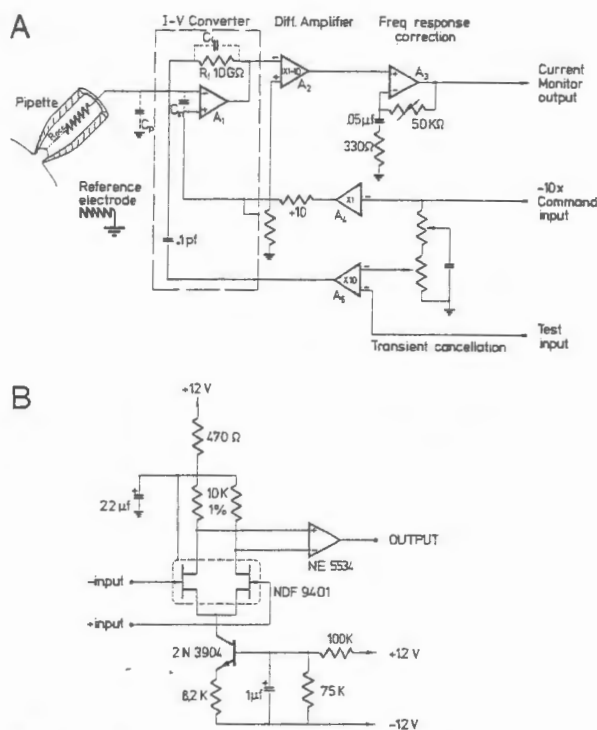


Fig. 4A and B. Circuit diagrams. (A) A simplified diagram of the recording system. The current-to-voltage converter is mounted on a micromanipulator, and the pipette holder (Fig. 1) plugs directly into it. Important stray capacitances (indicated by dotted lines) are the feedback capacitance $C_f \approx 0.1$ pF and the total pipette and holder capacitance $C_p = 4-7$ pF. C_{in} represents the input capacitance of amplifier A_1 , which is either a Burr Brown 3523J or the circuit shown in B. With the values shown, the frequency response correction circuit compensates for time constants $R_f C_f$ up to 2.5 ms and extends the bandwidth to 10 kHz. The transient-cancellation amplifier A_5 sums two filtered signals with time constants variable in the ranges 0.5–10 μ s and 0.1–5 ms; only one filter network is shown here. The test input allows the transient response of the system to be tested: a triangle wave applied to this input should result in a square wave at the output. Amplifiers A_2 , A_4 and A_5 are operational amplifiers with associated resistor networks. The op amps for A_2 and A_4 (NE 5534, Signetics or LF 356, National Semiconductor) are chosen for low voltage noise, especially above 1 kHz; more critical for A_3 and A_5 (LF 357 and LF 356) are slew rate and bandwidth. For potential recording from whole cells (see part IV), a feedback amplifier is introduced between current monitor output and the voltage command input. (B) Circuit of a low-noise operational amplifier for the $I-V$ converter with a selected NDF9401, dual FET (National Semiconductor) and the following approximate parameters: Input bias current, 0.3 pA; input capacitance, 8 pF; voltage noise density at 3 kHz, 5×10^{-17} V 2 /Hz; and gain-bandwidth product 20 MHz. The corresponding values for the 3523J are 0.01 pA, 4 pF, 4×10^{-16} V 2 /Hz and 0.6 MHz. The lower voltage noise of this amplifier is apparent in the $I-V$ converter's background noise above 500 Hz. The high gain-bandwidth product of the amplifier results in a loop bandwidth of ≈ 300 kHz in the $I-V$ converter, so that the frequency response in the 5–10 kHz region is negligibly affected by changes in C_p . The loop bandwidth with the 3523J is about 5 kHz

reduced in pipettes having steeper tapers near the tip, reducing R_{acc} , or having the coating extend closer to the tip, reducing C_{tip} .

Noise in the Current-to-Voltage Converter. Figure 4A shows a simplified diagram of the recording electronics. The pipette current is measured as the voltage drop across the high-valued

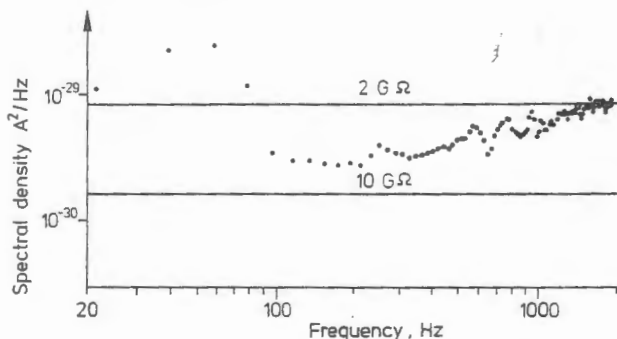


Fig. 5. Power spectrum of the total background noise from a rat myoball membrane patch at resting potential (dots). The amplifier of Fig. 4B was used, with a coated, hard-glass pipette. The patch resistance was 50 G Ω . Lines indicate the lower limit of the noise imposed by the 10 G Ω feedback resistor, and for comparison, the Johnson noise in a 2 G Ω resistor

resistor R_f ; the Johnson noise in this resistor is the predominant noise source in the $I-V$ converter below a few hundred Hertz. The substantial shunt capacitance $C_f \approx 0.1$ pF across this resistor affects the frequency response of the $I-V$ converter but makes no contribution to $Re\{Y\}$, and therefore to the noise current, assuming that it is a pure capacitance. This assumption appears to hold for the colloidfilm resistors (Type CX65, Electronic GmbH, Unterhaching/Munich, FRG) we use, since, after correction of the frequency response, we found that the $I-V$ converter's noise spectrum was unchanged when we substituted a homemade tin-oxide resistor having $C_f < 0.01$ pF for the commercial resistor. Other resistor types, including the conductive-glass chip resistors we have previously used (Neher et al. 1978) and colloid-film resistors with higher values do not show the transient response characteristic of a simple $R-C$ combination and therefore probably have a frequency-dependence of $Re\{Y\}$. Correcting the frequency response of these resistors is also more complicated; this is the primary reason why we have not yet used values for R_f above 10 G Ω , even though this might improve the low-frequency noise level.

The other main noise source in the $I-V$ converter is the operational amplifier itself. With both of the amplifiers we use (Burr Brown 3523J, and the circuit of Fig. 4B) the low-frequency (4–100 Hz) spectral density is essentially equal to the value expected from R_f , suggesting that the amplifier current noise is negligible. At higher frequencies however the amplifier voltage noise becomes the dominant noise source. This voltage noise is imposed by the feedback loop on the pipette and the input of the amplifier, causing a fluctuating current to flow through R_f to charge C_p and C_{in} (see Fig. 4). The resulting contribution to the current fluctuations has the spectrum

$$S_I(f) = [2\pi f(C_p + C_{in})]^2 S_{V(A)}(f), \quad (4)$$

where $S_{V(A)}$ is the amplifier voltage noise spectral density. The f^2 -dependence dominates over the constant or $1/f$ behavior of $S_{V(A)}$ giving an increase of S_I with frequency. This noise source can be reduced by minimizing C_p by using a low solution level and avoiding unnecessary shielding of the pipette and holder. It can also be reduced by choosing an operational amplifier having low values for C_{in} and $S_{V(A)}$; the amplifier of Fig. 4B was designed for these criteria.

Figure 5 shows the spectrum of the background noise during an actual experiment. Because the noise variance is the

integral of the spectrum the high-frequency components have much greater importance than is suggested by this logarithmic plot. Below 90 Hz the excess fluctuations mainly come from 50 Hz pickup. In the range 100–500 Hz the spectral density is near the level set by the 10 G Ω feedback resistor. Above 500 Hz, electrode noise sources and the amplifier voltage noise contribute about equally to the rising spectral density.

Capacitance Transient Cancellation. For studying voltage-activated channels voltage jumps can be applied to the pipette. However, a step change in the pipette potential can result in a very large capacitive charging current. For example, charging 5 pF of capacitance to 100 mV in 5 μ s requires 100 nA of current, which is 4–5 orders of magnitude larger than typical single channel currents. We use three strategies to reduce this transient to manageable sizes. First, we round the command signal (e.g. with a single time constant of 20 μ s) to reduce the peak current in the transient. Second, we try to reduce the capacitance to be charged as much as possible. Metal surfaces near the pipette and holder (excepting the ground electrode in the bath!) are driven with the command signal; this includes the microscope and stage, and the enclosure for the $I-V$ converter. (Alternatively, an inverted command signal could be applied only to the bath electrode.) This measure reduces the capacitance to be charged to 1–2 pF when coated pipettes and low solution levels are used. Notice, however, that while the capacitance to be charged by an imposed voltage change is reduced, C_p is unchanged for the purpose of the noise calculation (Eq. 4).

Third, we use a transient cancellation circuit which injects the proper amount of charge directly into the pipette, so that the $I-V$ converter is required to supply only a small error current during the voltage step. The charge is injected through a small, air-dielectric capacitor (see Fig. 4A) which is driven with an amplified and shaped version of the command voltage. The same capacitor can be used to inject currents for test purposes. With these three measures the transient from a 100 mV step can be reduced to below 10 pA (at 2 kHz bandwidth), which is small enough to allow computer subtraction of the remainder.

Part II

Patch Current Recording with Giga-Seals

1. Development of the Giga-Seal

In the past, seal resistances as high as 200 M Ω could be obtained by pressing a pipette tip against a cell membrane and applying suction. This same procedure can also lead to the formation of a seal in the gigaohm range; the only difference is that precautions must be taken to ensure the cleanliness of the pipette tip (Neher 1981). The main precautions are (1) the use of filtered solutions in the bath as well as in the pipette; and (2) using a fresh pipette for each seal. Further precautions are listed below.

The formation of a giga-seal is a sudden, all-or-nothing increase in seal resistance by as much as 3 orders of magnitude. Figure 6 shows the time-course of the development of a 60 G Ω seal in the perisynaptic region of a frog muscle fibre. When the tip of the pipette was pressed against the enzymatically cleaned muscle surface the seal resistance was 150 M Ω . (The resistance was measured by applying a 0.1 mV voltage pulse in the pipette and monitoring the

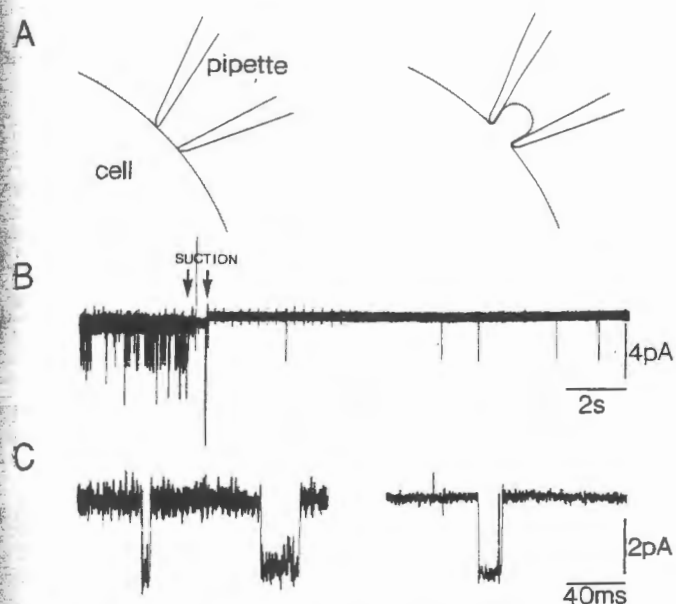


Fig. 6A—C. Giga-seal formation between pipette tip and sarcolemma of frog muscle. (A) Schematic diagrams showing a pipette pressed against the cell membrane when the pipette-membrane seal resistance is of the order of 50–100 Megohms (*left*), and after formation of a giga-seal when a small patch of membrane is drawn into the pipette tip (*right*). (B) The upper trace is a continuous current record before, during and after application of suction. In this experiment a pipette-membrane seal resistance of 150 M Ω was achieved by pressing the pipette against the membrane. Single suberyldicholine-induced channel currents are apparent. During the time indicated by the two arrows slight suction was applied to the pipette interior resulting in the formation of a giga-seal of 60 G Ω resistance. Note reduction in background noise level. The decrease in channel opening frequency presumably resulted from depletion of agonist in the pipette tip during suction. It increased again during the minute following giga-seal formation. The two large current deflections represent artifacts. The lower traces show single channel currents at higher resolution before (*left*) and after (*right*) formation of a giga-seal. The single channel current pulse on the right is preceded by capacitive artifacts from a calibration pulse. All records were made at the cell's resting potential of -92 mV and at 11°C . They were low pass filtered at 1 kHz (*upper trace*) or 3 kHz (*lower traces*)

resulting current flow). When a slight negative pressure of 20–30 cm H₂O was applied (arrows) the resistance increased within a few seconds to 60 G Ω . The development of giga-seals usually occurs within several seconds when a negative pressure is applied; seals always remain intact when the suction is subsequently released. In some cases giga-seals develop spontaneously without suction. In other cases suction has to be applied for periods of 10–20 s, or a seal may develop only after suction has been released.

It was previously suggested that upon suction the membrane at the pipette tip is distorted and forms an Ω -shaped protrusion (Neher 1981). This is indeed supported by measurements of patch capacitance after giga-seal formation (Sigworth and Neher 1980). The increase in area of glass-membrane contact, going along with such a distortion, probably explains the gradual, 2–4-fold increase of seal resistance which is usually observed during suction shortly before giga-seal formation, and is also seen in cases when giga-seals do not develop. Giga-seal formation, however, is unlikely to be explained solely by such an area increase. Crude estimates of the thickness of a water layer interposed between membrane and glass give values in the range 20–50 Å for

values of the seal resistance between 50 and 200 M Ω . These distances are characteristic for equilibrium separations between hydrophilic surfaces in salt solutions (Parsegian et al. 1979; Nir and Bentz 1978).

A seal resistance larger than 10 G Ω , however, is consistent only with glass-membrane separations of the order of 1 Å, i.e. within the distance of chemical bonds. The abrupt change in distance involved may therefore represent the establishment of direct contact between the surfaces, as occurs during transfer of insoluble surface monolayers on to glass substrates (Langmuir 1938; Petrov et al. 1980).

Also in favor of a tight membrane-glass contact is evidence that small molecules do not diffuse through the seal area. After establishment of a giga-seal the application of high ACh concentrations (in the range of 5–10 μM) outside the pipette does not activate single channel currents in the patch, even though the rest of the cell is depolarized by 20–50 mV.

The high-resistance contact area between glass and membrane also seems to be well delineated. We conclude this from the observation that the so-called "rim-channel" currents, which are quite common when using thick-walled pipette tips, are rarely observed after formation of a giga-seal (see below).

Reproducibility of Giga-Seals. The success rate for the establishment of giga-seals varies for different batches of patch pipettes. This variability probably results from a combination of several factors. The following general rules have been found helpful so far.

1. To avoid dirt on the pipette tip, pipettes should always be moved through the air-water interface with a slight positive pressure (10 cm H₂O). Even the first pipette-cell contact should be made with pipette solution streaming outwards. When the pressure is released while the pipette touches the cell the pipette membrane seal resistance should increase by a factor > 2 .

2. Each pipette should be used only once after positive pressure has been relieved.

3. Following enzyme treatment of muscle preparations the surface of the bathing solution is frequently covered with debris which readily adheres to the pipette tip, preventing giga-seal formation. The water surface can be cleaned by wiping with lens paper or by aspiration.

4. HEPES-buffered pipette solutions should be used when Ca²⁺ is present in the pipette solution. In phosphate buffer small crystals often form at the pipette tip by precipitation.

5. When slightly (10%) hypoosmolar pipette solutions are used the giga-seals develop more frequently. With these precautions, about 80% of all pipettes will develop giga-seals on healthy preparations. However, even after giga-seal formation, irregular bursts of fast current transients are observed on some patches. We interpret these as artifacts due to membrane damage or leakage through the seal.

2. Improved Current Recording After Giga-Seal Formation

When a pipette is sealed tightly onto a cell it separates the total cell surface membrane into two parts: the area covered by the pipette (the patch area) and the rest of the cell. Current entering the cell in the patch area has to leave it somewhere else. Thus, the equivalent circuit of the whole system consists of two membranes arranged in series. This, and the resulting complications will be discussed in a later section (see also Fig. 10). Here we will focus on the simple case that the total cell membrane area is very large with respect to the patch area.

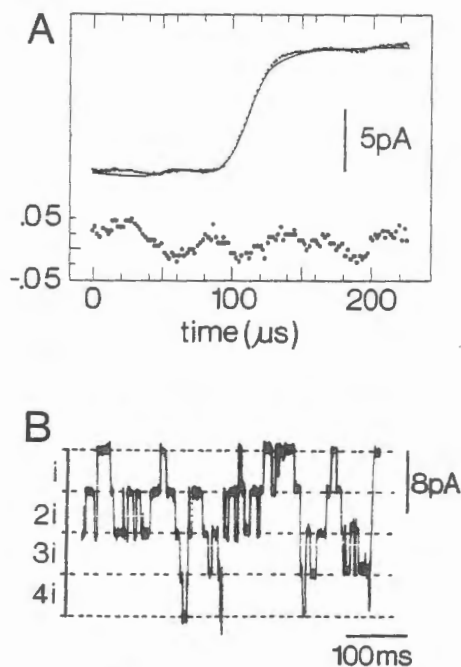


Fig. 7A and B. Demonstration of time resolution and of uniformity in step sizes. (A) A digitized record (1.87 μ s sample interval) of the opening time course of channels activated by 100 nM SubCh on the perisynaptic region of an adult frog muscle fiber (11°C). The patch was hyperpolarized to approximately -160 mV and a solution containing 100 mM CsCl was used. The single channel currents were -10.5 pA in amplitude. Six individual channel opening events were averaged by superposition after alignment with respect to the midpoint of the transition. The same procedure was followed to obtain the instrument's step-response, using records from capacitively-injected current steps. The step response (continuous line) is superimposed on the channel's opening time course after amplitude scaling. The relative difference between the two curves is plotted below. The amplitude of the fluctuations in the difference record is the same during the transition and during the rest of the record. Based on the size of these fluctuations, an upper limit was estimated for the transition time between the closed and open states of the channel by the following procedure: The transfer function of the electronic apparatus was calculated from the known step response by Fourier transform methods. Then, theoretical responses to open-close transitions of various shapes were calculated and compared to the experimental step response. It was found that the predicted deviations between the two curves were significantly larger than the observed ones only when the open-close transitions were spread out in time over 10 μ s or more. (B) A current record from a myoball under the following conditions: 1 μ M ACh; 18°C; -140 mV holding potential. Individual single channel currents superimpose to form regularly spaced amplitude levels

Then, the small patch currents will not noticeably alter the cell's resting potential. For instance, a myoball with 50 M Ω input resistance will be polarized less than 0.5 mV by a patch current of 10 pA. Thus, a patch can be considered "voltage clamped" even without the use of intracellular electrodes. The clamp potential is equal to the difference between the cell potential and the potential in the pipette. Some properties of current recordings done under this type of "voltage clamp" are illustrated here.

a) Increased Amplitude and Time Resolution; the Time Course of Channel Opening is Fast. Due to low background noise and an improved electronic circuit the time course of channel opening and closing can be observed at 5–10 kHz resolution. Figure 7A illustrates the average opening time-course of suberyldicholine-activated channels at the frog endplate

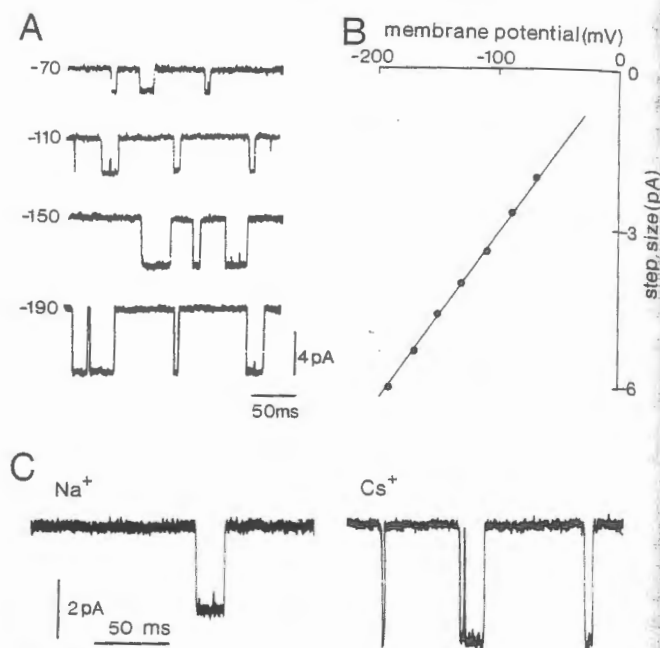


Fig. 8A–C. Control of voltage and of ionic environment in the pipette tip after formation of a giga-seal. (A) Single channel current recordings at 50 nM SubCh in the perisynaptic membrane of cutaneous pectoris muscle fibre; 11°C. The membrane potential of this fibre was -89 mV measured by an intracellular microelectrode. The pipette potential was shifted by different amounts to obtain the membrane potential indicated on the left of each trace (in mV). The pipette was filled with Ringer solution in which NaCl concentration was reduced to 100 mM to improve giga-seal formation. (B) Current-voltage relationship of channel currents, derived from the experiment shown in A. Each point represents the mean current amplitude of ten individual current events. The straight line is drawn by eye and represents a single channel (chord) conductance of 32 pS. (C) Single channel current recordings under the conditions of part A at -90 mV membrane potential. The main salt in the pipette solution was 100 mM CsCl (right) and 100 mM NaCl (left). The average single channel current amplitudes were 2.8 pA and 3.8 pA in Na⁺ and Cs⁺ solutions respectively

region. The large single channel currents and the low background noise level allowed a much higher time resolution to be obtained than in previous recordings. Still, the rising phase of the conductance (dotted line) is seen to be indistinguishable from the step response of the measuring system (continuous line). From a comparison of the two time courses it can be estimated that the actual channel opening occurs within a time interval smaller than 10 μ s (see legend, Fig. 7).

b) Lack of Rim-Channel Currents. A major problem of the extracellular patch clamp technique has been the occurrence of currents from channels in the membrane area under the rim of the pipette. These currents are not uniform in size; the resulting skewed step-size histograms complicate the estimation of the single channel current amplitudes (Neher et al. 1978). Current recordings with giga-seals, however, show amplitude distributions that are nearly as narrow as expected from noise in the baseline. The improvement reflects a more sharply delineated seal region. A recording is shown in Fig. 7B which demonstrates the regularity in current amplitudes.

The regularity also allows (i) the unequivocal discrimination between channel types of slightly different con-

ductance, e.g. synaptic and extrasynaptic ACh receptor channels, and (ii) analysis of channel activity when the currents of several channels overlap.

c) *Voltage Control of the Membrane Patch.* Previously the potential inside the pipette had to be balanced to within less than 1 mV of the bath potential; otherwise large, noisy leakage currents flowed through the seal conductance. The high seal resistance now allows the patch membrane potential to be changed. For example, a 100 mV change in pipette potential will drive only 5 pA of current through a 20 G Ω seal. This leakage is comparable in size to a single channel current and is easily manageable by leakage subtraction procedures. The ability to impose changes in membrane potential has been used to activate Na channels in myoballs (Sigworth and Neher 1980). It also allows measurement of single channel currents in adult muscle fibres over a wide range of potential that is not accessible with the conventional two-microelectrode voltage clamp because of local contractions. Figure 8A and B shows representative traces and the current-voltage relationship of single channel currents recorded from a muscle fibre at various patch membrane potentials ranging from -70 to -190 mV.

d) *Control of Extracellular Ion Composition.* Giga-seals form a lateral diffusion barrier for ions (see above, p. 91). Here we show that the ionic composition on the external side of the patch membrane is that of the pipette solution. Figure 8C illustrates ACh-activated single channel currents from a frog muscle fibre when the major salt in the pipette was CsCl (100 mM) while the bath contained normal Ringer. The open channel conductance was seen to be 1.3 times larger than the conductance in standard Ringer solution, consistent with the larger estimates of conductance that have been made from fluctuation analysis (Gage and Van Helden 1979).

Part III

Single Channel Current Recording from "Cell-Free" Membrane Patches

Apparently the contact between cell membrane and glass pipette after formation of a giga-seal is not only electrically tight, but also mechanically very stable. The pipette tip can be drawn away from the cell surface without a decrease in the seal resistance (Hamill and Sakmann 1981; Neher 1981). As will be shown below a tight vesicle sealing off the tip forms, when this is done in normal Ca²⁺-containing bath solution. Procedures are described by which the resistance of either the inner or the outer part of the vesicle can be made low (< 100 M Ω) without damaging the giga-seal. The remaining intact membrane can then be studied as before. Either "inside-out" or "outside-out" patches can be isolated in this way (see Fig. 9). By varying the composition of the bath solution, the effect of drugs or ion concentration changes on single channel currents can be studied at either the cytoplasmic or the extracellular face of the membrane.

1. Vesicle Formation at the Pipette Tip

The top trace in Fig. 10A shows single channel currents recorded in a frog muscle fibre at its resting potential of -90 mV. The patch pipette was filled with standard Ringer solution plus 50 nM suberyldicholine (SubCh) and was sealed against the surface membrane in the perisynaptic region. When the pipette tip was slowly withdrawn a few μ m from the

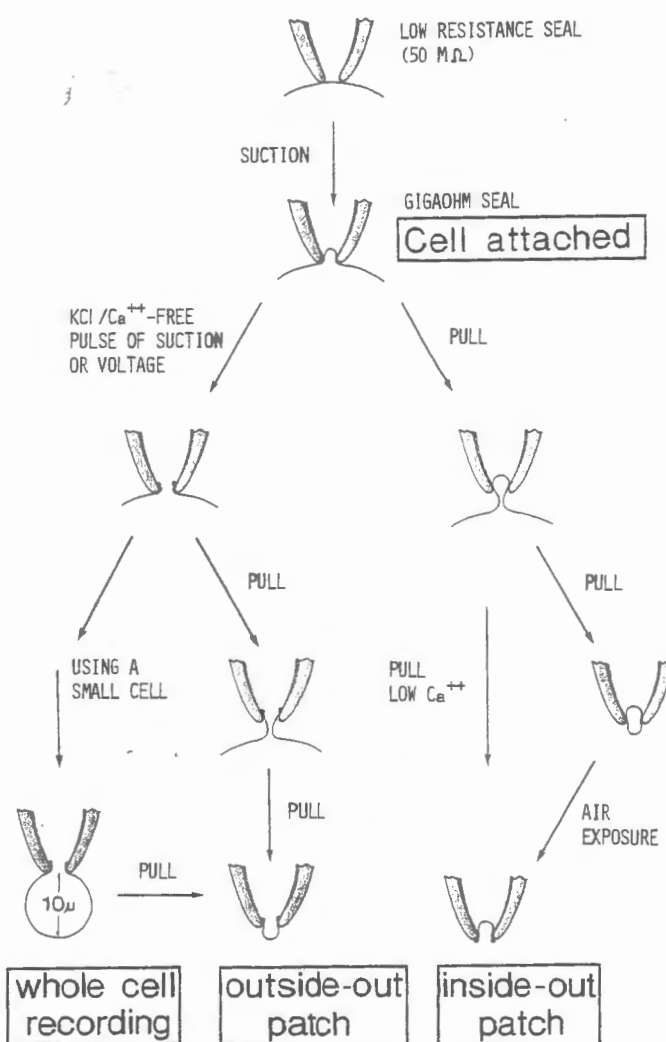


Fig. 9. Schematic representation of the procedures which lead to recording configurations. The four recording configurations, described in this paper are: "cell-attached", "whole-cell recording", "outside-out patch", and "inside-out patch". The upper most frame is the configuration of a pipette in simple mechanical contact with a cell, as has been used in the past for single channel recording (Neher et al. 1978). Upon slight suction the seal between membrane and pipette increases in resistance by 2 to 3 orders of magnitude, forming what we call a cell-attached patch. This configuration is described in part II of this article. The improved seal allows a 10-fold reduction in background noise. This stage is the starting point for manipulations to isolate membrane patches which lead to two different cell-free recording configurations (the outside-out and inside-out patches described in part III). Alternatively, voltage clamp currents from whole cells can be recorded after disruption of the patch membrane if cells of sufficiently small diameter are used (see part IV of this article). The manipulations include withdrawal of the pipette from the cell (pull), short exposure of the pipette tip to air and short pulses of suction or voltage applied to the pipette interior while cell-attached

cell surface the shape of single channel currents became rounded and they decreased in size (middle trace). Often a fine cytoplasmic bridge could then be observed between the cell surface and the pipette as shown in Fig. 10D. Upon further removal the cytoplasmic bridge tied off but left the giga-seal intact. Single channel currents further decreased in size and finally disappeared in the background noise within the next 1-2 min. The pipette input resistance remained high (110 G Ω , see bottom trace).

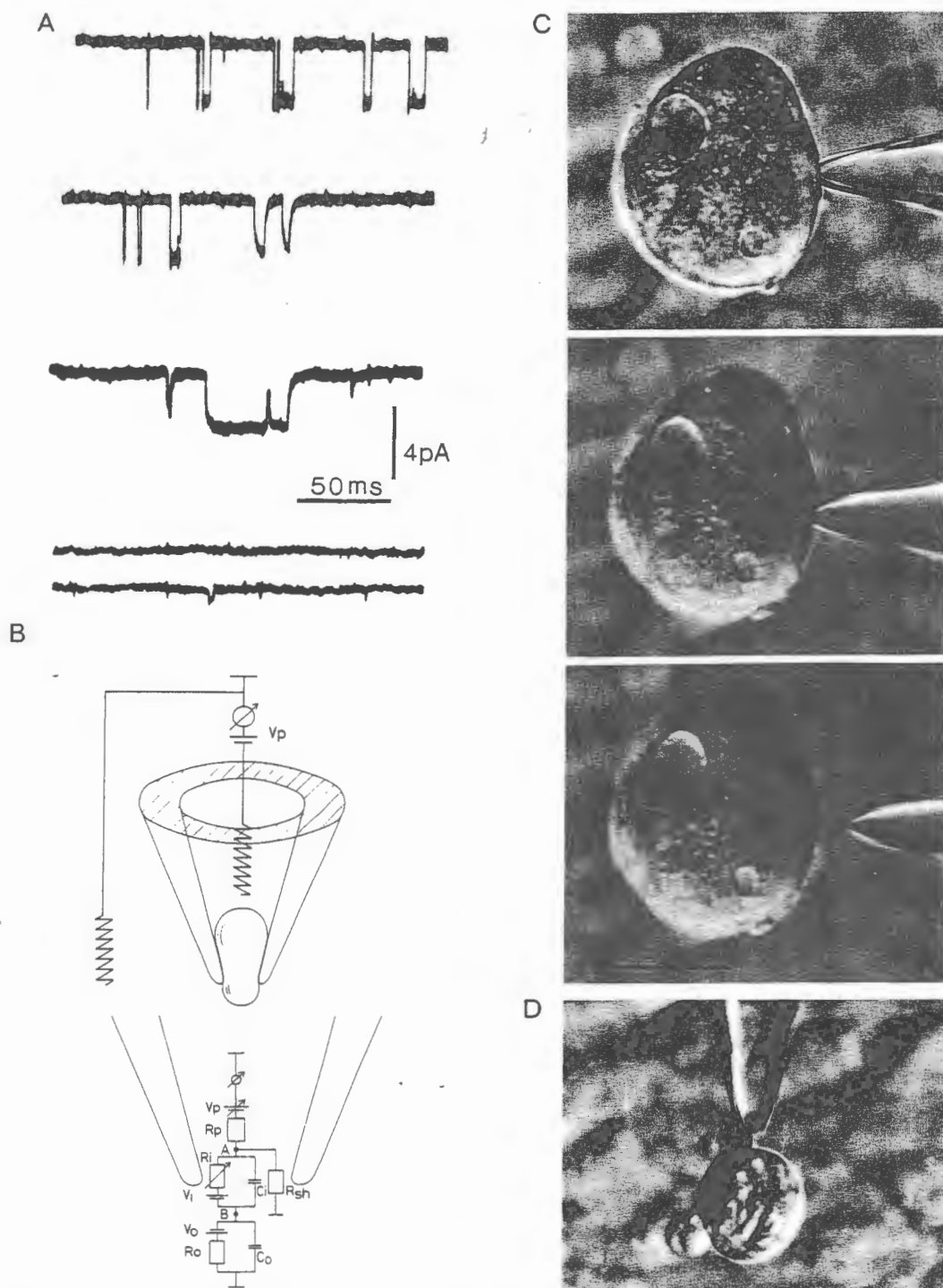


Fig. 10A–D. Formation of a membrane vesicle at the pipette tip. (A) Patch current recording during withdrawal of the pipette tip from muscle sarcolemma. The *upper trace* illustrates single channel currents after formation of a gigaseal under conditions similar to those of Fig. 8. During withdrawal of the pipette single channel currents suddenly appeared distorted in shape; currents showed rounded rising and falling time courses and progressively lower amplitudes. In this experiment single channel currents became undetectable within 30 s following the appearance of rounded current events. The pipette-membrane seal resistance remained high, ($> 30 \text{ G}\Omega$) and current pulses remained undetectable even after hyperpolarizing the membrane by 90 mV. This suggests that the pipette opening became occluded by a membranous structure, which most probably was a closed vesicle as illustrated in part B. (B) Schematic diagram of recording situation following formation of a membrane vesicle. The equivalent circuit is modelled by parallel current pathways through the shunt resistance R_{sh} and through the vesicle. The two halves of the vesicle are represented by $R-C$ combination in series. The inner membrane, exposed to the pipette solution, has resistance R_i and capacitance C_i . The outer membrane, represented by R_o and C_o , is exposed to the bath solution. Point B represents the interior of the vesicle. V_o and V_i are the electromotive forces of the outer and inner membranes. R_p is the access resistance of the unsealed pipette. Opening of a channel in the presence of ACh in the pipette solution decreases the resistance of the inner membrane, R_i . Therefore, R_i which in fact is a parallel combination of membrane resistance and open channel resistance R_c is modelled as a variable resistor. (C) Visualisation of membrane patch isolation from a rat myoball. The upper micrograph shows the tip of a patch pipette in contact with a myoball. When suction is applied, an Ω -shaped membrane vesicle is pulled into the pipette tip (*middle micrograph*). Following slight withdrawal of the pipette tip from the myoball, a cytoplasmic bridge of sarcolemma between pipette tip and myoball surface was observed (not shown). At this stage of membrane isolation distorted single channel current pulses are recorded like those shown in A. Upon further withdrawal the cytoplasmic bridge ruptures leaving a small vesicle protruding from the pipette tip (*lower micrograph*). Note “healing” of the sarcolemmal membrane of the myoball (D) Visualisation of cytoplasmic bridge between myoball and vesicle in the pipette tip in another experiment. Calibration bar: 20 μm . (Normarsk interference optics, $\times 40$ water immersion objective)

The most likely explanation for this sequence of events is that during rupture of the cytoplasmic bridge between pipette tip and cell surface a closed vesicle formed at the tip of the pipette. The formation of a vesicle is illustrated in Fig. 10C on a myoball. The vesicle is partly exposed to the bath solution ("outer membrane") and partly to the pipette solution ("inner membrane") in the way shown schematically in Fig. 10B.

Three kinds of observations give indications on the electrical properties of the vesicle. (i) When ACh is added at a low concentration to the bath solution, current pulses of reduced size are sometimes recorded at an applied pipette potential V_p of +90 mV or more. These current pulses reflect an outward current flow through AChR channels on the outer membrane of the vesicle. (ii) Destruction of the barrier properties of the outer membrane (see the next section) results in the reappearance of single channel currents through the inner membrane. (iii) In some experiments single channel currents of decreased amplitude and distorted shape could be recorded when the pipette potential was increased to $> +70$ mV even several minutes following pipette withdrawal. Examples of such distorted current pulses recorded from patches and vesicles are illustrated in Figs. 10A and 11. Single channel currents were of rectangular shape as long as the membrane patch was attached to the cell.

Equivalent circuit. The electrical signals after vesicle formation can be explained by an equivalent circuit shown in Fig. 10B. The two halves of the vesicle form a series combination of two RC-circuits, shunted by the leakage resistance R_{sh} . Assuming a specific conductance of the membrane of 10^{-4} Scm $^{-2}$ and an area of a semi-vesicle in the range of several μm^2 , values for the membrane resistances R_i and R_o should be in the range of several hundred G Ω , much larger than the resistance of a single open AChR-channel (about 30 G Ω). Local damage or partial breakdown of the membrane could bring this value down into the range of single open channels. Then, opening of a single channel in either of the two membranes would result in an attenuated current flow through the series combination. Consider the simple case that R_i and R_o are the same and are identical to the resistance of a single channel R_c . Then, upon opening of a single channel the apparent conductance at steady state is attenuated by a factor of 6 with respect to the true conductance.

More generally, the apparent conductance G_{app} of a single channel (assumed to open on the inner side of the vesicle)

$$G_{app} = R_c^2 / ((R_i + R_o)(R_c R_o + R_c R_i + R_i R_o)).$$

The time course will be governed by the time course of the voltage at point B in the equivalent circuit. For a combination of two RC-elements and a step-like perturbation this will be a single exponential (neglecting R_p of Fig. 10B). The time constant τ of the exponential is equal to

$$\tau = R_c \parallel R_i \parallel R_o \cdot (C_i + C_o),$$

where $R_c \parallel R_i \parallel R_o$ is the parallel combination of R_c , R_i and R_o (see Fig. 10B). For the simple case above $\tau_1 = R_c(C_i + C_o)$ while the channel is open and $\tau_2 = R_c(C_i + C_o)/2$ while the channel is closed. The measurement of a time constant, therefore, gives the total membrane capacitance of the vesicle. More generally, determination of G_{app} , τ_1 , and τ_2 allows calculation of the three unknowns R_i , R_o and $(C_i + C_o)$. If the conductance of the single channel ($1/R_c$) is known, the analysis neglects the effects of R_{sh} , which however adds a constant offset in current (at $V_p = \text{constant}$ and $R_p \ll R_{sh}$).

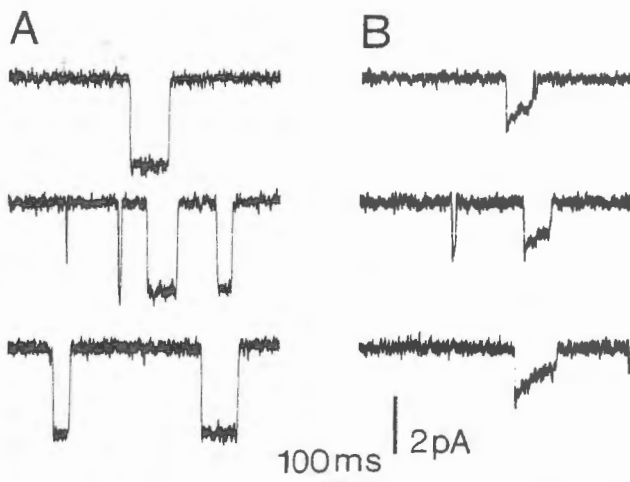


Fig. 11 A and B. Distorted single channel current shapes following isolation of a membrane vesicle from myoball sarcolemma. (A) Single channel currents recorded from a cell-attached membrane patch. In this experiment the Na^+ in the pipette solution was reduced to 50 mM. Pipette potential was +80 mV. Assuming a resting potential of -70 mV the membrane potential across the patch was -150 mV. The slope conductance was 21 pS. (B) Single channel currents after physical isolation of the membrane patch from the myoball. Pipette potential was +80 mV. Single channel currents could be observed at the pipette zero potential indicating that the vesicle had a membrane potential. The apparent slope conductance of the initial peak amplitude of these current events was 12 pS. All records filtered at 0.4 kHz, low pass; 18°C. The duration of the current events is not representative since long duration currents were selected to illustrate differences in the time course in cell-attached and cell-free configurations. Also, the time constant of decay was unusually long in this experiment. In some experiments single channel currents similar to those shown here but of very small amplitude could be observed also without application of a pipette potential. This indicates that the vesicle can have a resting potential.

Experimental data gave estimates for $C_i + C_o$ in the range 0.03 - 0.3 pF. Assuming a specific capacitance of the vesicle

The "Outside-Out" Membrane Patch Configuration. The outer membrane of the vesicle can be opened by mechanical rupture of the vesicle formation. Isolation of a membrane patch from the outside-out configuration is illustrated in Fig. 10C. A few minutes following the establishment of a gigaseal, background noise increased progressively by several orders of magnitude. This was accompanied by a decrease in the amplitude of the current pulses. The vesicle could produce a linear relationship between the stage axis and the current in Fig. 14A. The resulting curves are completely overlapping when the pipette is moved around the vesicle. For membrane mixtures of anionic and cationic lipids, the yield of stable recordings is provided by the fact that the site and in the bath were kept constant and their properties were obtained after successful patching and in the bath were kept constant. This is shown in Fig. 14B. The change in curvature and the fact that the vesicle contents between the interior of a vesicle and the bath immediately point towards very efficient equilibration between the interior of a vesicle and the bath. Ionic exchange across a disrupted membrane between the pipette interior and the cell interior was observed in whole cell recording configuration (see part IV). These findings, together, make it very likely that true equilibration

be done. When the outer membrane of the vesicle is disrupted the cytoplasmic face of the inner membrane is exposed to the bath solution. Its extracellular face is exposed to the pipette solution. We call this an "inside-out" membrane patch. When, on the other hand, the inner membrane of the vesicle is disrupted the cytoplasmic face of the outer membrane of the vesicle is exposed to the pipette solution, its extracellular face to the bath solution. This will be called an "outside-out" patch. The next two sections describe formation of these two configurations of membrane patches.

The "Inside-Out" Membrane Patch. To obtain a membrane whose cytoplasmic face is exposed to the bath solution, either formation of the outer vesicle membrane has to be prevented (Horn and Patlak 1980) or it has to be disrupted once it has been formed (Hamill and Sakmann 1981). This can be done either mechanically or chemically.

A prerequisite for isolated patch formation is a seal of $>20\text{ G}\Omega$. Disruption of the outer vesicle membrane is done by passing the pipette tip briefly through the air-water interface of the bath or by touching an air bubble held by a nearby pipette. Brief contact with a drop of hexadecane will sometimes disrupt the vesicle. Figure 12 illustrates the disruption of the barrier properties of the outer vesicle membrane. Initially the pipette tip was sealed against a myoball membrane. The pipette solution contained $0.5\ \mu\text{M}$ ACh. Single channel currents were recorded at the cell's resting potential as shown in the uppermost trace. After withdrawal of the pipette tip from the cell surface single channel currents disappeared. Upon increasing the pipette potential to $+70\text{ mV}$ the trace became noisier but single currents were not resolved. By briefly (1–2 s) passing the tip through the air-water interface the outer membrane of the vesicle was disrupted. Upon reimmersion of the tip into the bath solution single channel currents of the expected size were recorded (Fig. 12). Single channel currents, which in most membrane patches of myoballs fall into two classes (Hamill and Sakmann 1981) were similar in their respective amplitudes in the cell-attached and cell-free configuration as shown in Fig. 12B on another patch at -100 mV membrane potential.

The outer membrane of the vesicle can also be made leaky by exposing it to a Ca-free, 150 mM KCl bath solution during isolation, as was originally used by Kostyuk et al. (1976) to disrupt neuronal membranes for internal dialysis. A vesicle tends to reform with this procedure, and mechanical disruption is usually required in addition to open the vesicle completely. The stability of inside-out patches is greatly improved when most of the Cl^- in the bath solution is replaced by SO_4^{2-} . For membrane patches isolated from myoballs an anion mixture of 4 mM Cl^- and 75 mM SO_4^{2-} was found to yield stable recordings for up to several hours.

The "Outside-Out" Membrane Patch. In order to work with the outer membrane of the vesicle, the inner membrane can be made leaky or can be disrupted in very much the same way as described for the case above, i.e. by exposing the inner vesicle membrane to a pipette solution containing 150 mM KCl and only a low ($<10^{-6}\text{ M}$) concentration of Ca. Alternatively it can be opened by mechanical rupture of the patch preceding vesicle formation. Isolation of a membrane patch in the outside-out configuration is illustrated in Fig. 13. A pipette containing 150 mM KCl and 3 mM HEPES buffer was used. A few minutes following the establishment of a giga-seal, the background noise increased progressively by several orders of magnitude. This was accompanied by a decrease of the

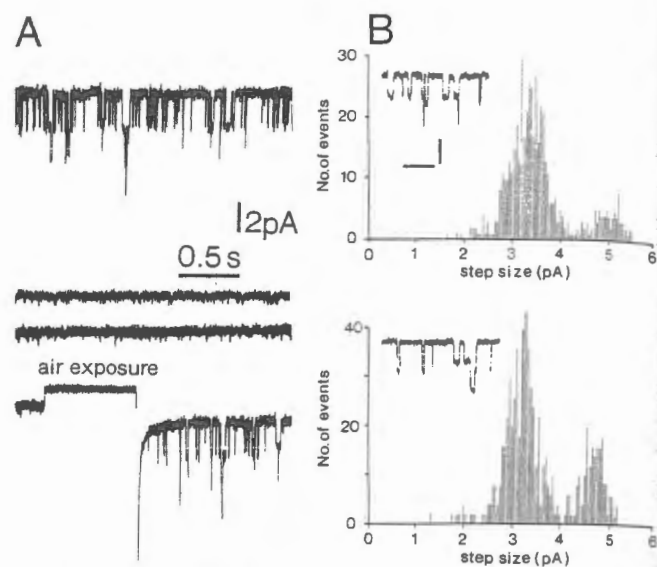


Fig. 12 A and B. Isolation of an "inside-out" membrane patch from rat myoball sarcolemma. (A) The upper three traces were recorded during the process of vesicle formation and are analogous to those shown in Fig. 10A. Standard solutions were used. The pipette contained $0.5\ \mu\text{M}$ ACh. Single channel currents (first trace, recorded at the cell's resting potential of $\sim -70\text{ mV}$) became undetectable following withdrawal of the pipette tip. Upon shifting the pipette potential from 0 (second trace) to $+70\text{ mV}$ (third trace) the current trace changed by only 0.8 pA , indicating formation of a closed vesicle where $R_o > R_i$ (see Fig. 10B). The pipette tip was then passed briefly (1–2 s) through the air-water interface which disrupted the outer membrane of the vesicle. Upon reimmersion single channel currents were recorded at a pipette potential of $+70\text{ mV}$ (fourth trace), which were similar to those of the cell-attached case (shown in the first trace). (B) Step size distribution of single channel currents recorded from the same patch of membrane in the cell-attached configuration (upper graph) and in the cell-free "inside-out" configuration (lower graph), both at a membrane potential of -100 mV . The pipette solution contained $0.5\ \mu\text{M}$ ACh. The distribution of step sizes is doubly peaked. It indicates that in this patch two types of AChR channels, junctional and extrajunctional, with slightly different open channel conductances were activated. The larger spread of step size distributions in the cell-attached recording configuration is due to the larger background noise which in this experiment was mostly caused by mechanical instabilities and which disappears following isolation of the patch. In some experiments the average opening frequency of AChR channels decreased (up to 30%) following isolation of the membrane patch. This is probably due to a decrease of the inner membrane area exposed to the pipette solution. Insets show examples of single channel current events (Calibration bars: 4 pA and 50 ms). A downward deflection of the current trace in this and all other figures indicates cation transfer from the compartment facing the extracellular membrane side to the compartment facing the cytoplasmic side. This is from the pipette to the bath solution for an inside-out patch.

pipette-bath resistance to less than $1\text{ G}\Omega$ and by the development of a large inward current. Upon withdrawal of the pipette tip from the cell surface the background noise decreased within 1–2 s to the initial low level and the pipette-bath resistance simultaneously increased to a value larger than $10\text{ G}\Omega$.

We attribute the initial decrease of the pipette input resistance to the disruption of the membrane patch and not to an increased leakage of the pipette-membrane seal. This follows from the observation that the inward current inverts at a rather large negative pipette potential presumably equal to the cell resting potential. Also the pipette input capacitance shows an increase corresponding to the cell capacitance (see below, Part IV).

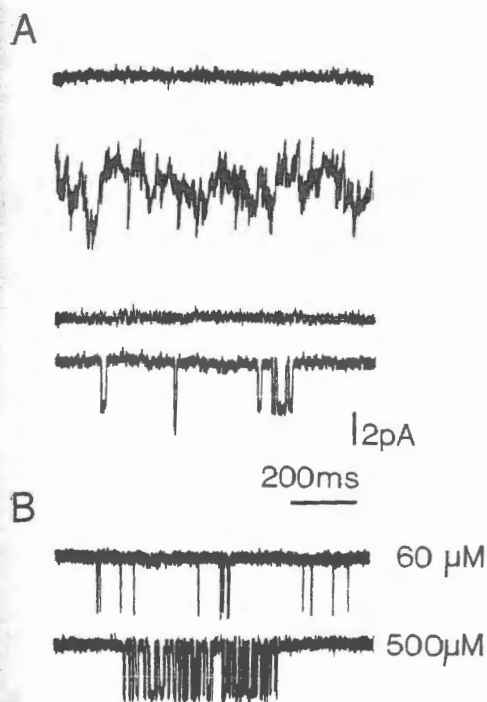


Fig. 13A and B. Isolation of an "outside-out" membrane patch from rat myoball sarcolemma. (A) After formation of a "gigaseal" using a pipette containing 150 mM KCl and 3 mM HEPES at pH 7.2 the background noise increased within 2–3 min. The upper two traces represent recordings immediately following gigaseal formation and 3 min later. At this stage a leakage current of > 1 nA developed which eventually drove the feedback amplifier into saturation. The leakage currents could be reduced or inverted when the pipette potential was shifted to -50 to -70 mV. The pipette access resistance decreased to values < 100 M Ω . Upon withdrawal of the pipette tip the pipette access resistance increased again into the G Ω range, and the background noise decreased (third trace). Addition of 0.5 – 1 μ M ACh to the bath solution induced single channel currents of 2.5 pA amplitude at -70 mV membrane potential (fourth trace). All records are filtered at 0.5 kHz; temp. 18° C. (B) Demonstration of equilibration of bath-applied agonists at the extracellular face of an outside-out patch. Single channel currents were recorded at -70 mV membrane potential from the same membrane patch when either 60 μ M carbachol (above) or 500 μ M carbachol (below) was added to the bath solution. At the lower concentration single channel current events appeared at random, at the higher concentration current pulses appeared in "bursts". Addition of 10^{-6} M α -BuTx irreversibly blocked agonist activated currents (not shown)

The subsequent sealing observed when pulling away the pipette apparently results from the formation of a new membrane bilayer at the pipette tip, with its external side facing the bath solution (outside-out patch, see Fig. 9). Several observations lead to this conclusion: (i) Air exposure of the pipette tip as described in the previous section results in a decrease of the pipette-bath resistance to values < 100 M Ω . (ii) Addition of low ACh concentrations to the bath solution activates single channel current pulses. At a pipette potential of -70 mV they are similar in their amplitude and average duration to those observed on cell-attached membrane patches (Fig. 13A). (iii) In experiments where only the pipette contained ACh, no single channel currents were recorded at this stage.

The breakdown of the initial membrane patch, which was spontaneous in the experiment illustrated in Fig. 13A, can be accelerated or initiated by applying brief voltage (of up to

200 mV) or negative pressure pulses (matching the pressure of a 100 cm H₂O column) to the pipette interior. In this way, the access resistance can be lowered to a value near the pipette resistance.

The extracellular face of outside-out membrane patches equilibrates rapidly (< 1 s) and reversibly with ACh added to the bath solution by perfusion of the experimental chamber or applied by flow of ACh-containing solution from a nearby pipette of 20 – 50 μ m tip diameter. Figure 13B shows a recording of single channel currents from an outside-out patch when carbachol is applied at 60 μ M and 500 μ M. At the low carbachol concentration current pulses appear at random intervals, whereas bursts of current pulses are recorded at high agonist concentration as previously reported for cell-attached membrane patches (Sakmann et al. 1980).

3. Equilibration of the Cytoplasmic Face of Cell-Free Patches with Bath or Pipette Solutions

In the previous two sections it was shown that by suitable manipulations either the inner membrane or the outer membrane of the vesicle can be disrupted such that it represents a low series resistance. In order to check whether, using either of the two configurations of cell-free membrane patches, the cytoplasmic face of the patch equilibrates with the experimental solution we have measured I – V relations of ACh-activated channels under various ionic conditions in both inside-out and outside-out configurations (Fig. 14A). The I – V relations show the following features which are expected for ionic equilibration between the cytoplasmic membrane face and the bath solutions or pipette solutions: (i) when Na⁺ concentration is reduced on one side of the membrane, one branch of the I – V relation changes strongly whereas the other branch is minimally affected in its extremes (ii) the two recording configurations result in overlapping I – V relationships when ionic compositions on both sides of the membrane are the same (iii) changes in the shape of the I – V relations can be reversed and are reproducible from one patch to the next.

It is well established that the disrupted membrane of the vesicle does not represent an appreciable electrical series resistance (see for instance Fig. 12). However it might well contribute to changes in the I – V relation if its conductance were high, but ion-selective. In such a case a potential would develop across the disrupted membrane which would produce a parallel shift in the I – V relation along the voltage axis. This, however, is contrary to the results shown in Fig. 14A where changes occur in curvature, and neighbouring curves approach each other asymptotically.

Further evidence for ionic equilibration is provided by kinetic studies. It was found that after successful patch isolation the I – V relations did not change their properties with time if solutions in the pipette and in the bath were kept constant. Furthermore steady state properties were obtained instantaneously upon a change of environment. This is shown in Fig. 14B.

Both the changes in curvature and the fact that the changes occur instantaneously point towards very efficient exchange of ionic contents between the interior of a vesicle and the compartment neighbouring its disrupted membrane. In addition, ionic exchange across a disrupted membrane between the pipette interior and the cell interior was observed in the whole cell recording configuration (see part IV). These findings, together, make it very likely that true equilibration

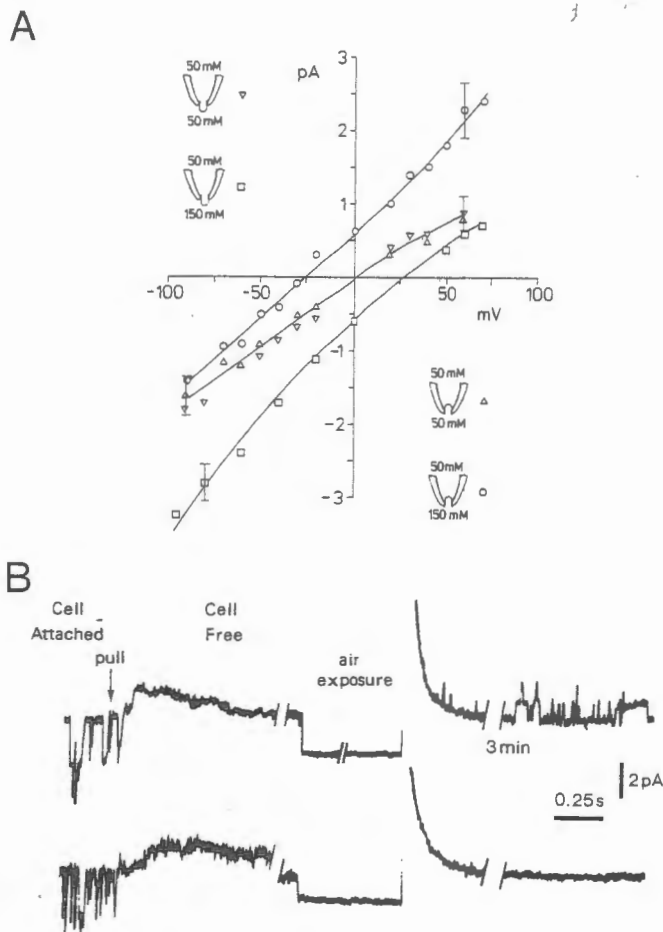


Fig. 14A and B. Equilibration of the cytoplasmic face of cell-free membrane patches with bath or pipette solutions. (A) $I-V$ relationships for acetylcholine-activated channels in inside-out and outside-out membrane patches measured under different ionic conditions. For all measurements the pipette solution contained 50 mM NaCl as the predominant salt. The bath solution contained initially 150 mM NaCl, which was changed to a solution containing 50 mM after patch isolation. Note that under symmetrical conditions $I-V$ relationships in both patch configurations overlapped, passed through the pipette zero potential, and showed slight rectification. Under asymmetrical conditions the reversal potentials were shifted by 25 mV. The $I-V$ relationships showed the expected curvature, and, in one branch each, approached the neighbouring symmetrical $I-V$. The symbols \circ , Δ , ∇ , \square represent the mean channel currents determined from 16, 3, 2, and 3 separate experiments. SEM's are shown for some averages. All measurements were made at 18°C. Changes in junction potentials caused by solution changes were measured independently, and were corrected for. (B) Current records before, during, and after formation of an inside-out patch at zero pipette potential. For both upper and lower traces the pipette was withdrawn from the cell while in normal bath solution. The pipette solutions contained 50 mM NaCl. During withdrawal of the pipette from the myoball, ACh-activated currents, evident while cell-attached, disappeared. For the upper trace the pipette tip was briefly exposed to air, and then returned to the normal bath solution. Inverted currents immediately appeared consistent with the vesicle being opened to the bath solution. The currents recorded did not change their properties over a three-min period. They displayed an $I-V$ relation similar to the inside-out asymmetrical case described in part A. For the lower trace, after pipette withdrawal from the cell, the bath solution was changed to one containing 50 mM NaCl and the pipette tip was then exposed shortly to air. No ACh-induced currents were evident at the pipette zero potential. They appeared upon polarization and displayed a similar $I-V$ relationship as described for symmetrical cases in part A.

between the cytoplasmic membrane face and adjacent bulk solutions takes place.

Part IV

Recording of Whole-Cell Voltage Clamp Currents

It was pointed out above that the membrane patch which separates the pipette from the cell interior can be broken without damaging the seal between the pipette rim and the cell membrane. This is the situation occurring at the initial stage during the formation of outside-out patches (see p. 96). Here, we demonstrate the suitability of this configuration for studying the total ionic currents in small cells. The technique to be described can be viewed as a microversion of the internal dialysis techniques originally developed for molluscan giant neurons (Krishtal and Pidoplichko 1975; Kostyuk and Krishtal 1977; Lee et al. 1978) and recently applied to mammalian neurones (Krishtal and Pidoplichko 1980). As it is appropriate only for cells of less than 30 μm in diameter, we take as an example bovine chromaffin cells in short-term tissue culture. These cells have a diameter of 10–20 μm . Their single channel properties will be detailed elsewhere (Fenwick, Marty, and Neher, manuscript in preparation).

The pipette was filled with a solution mimicking the ionic environment of the cell interior (Ca-EGTA buffer, high K^+). After establishment of a giga-seal, the patch membrane was disrupted, usually by suction, as previously described (see above). The measured zero-current potential was typically -50 to -70 mV. This corresponds to the cell resting potential (Brandt et al. 1976). Applying small voltage jumps from this potential revealed a resistance value in the range of 10 $\text{G}\Omega$. This resistance is mainly due to the cell membrane since markedly larger resistances (20–50 $\text{G}\Omega$) were obtained when using a CsCl solution in the pipette interior and tetrodotoxin in the bath. Small voltage jumps also showed that the disruption of the initial patch is accompanied by a large increase of the input capacitance (Fig. 15). The additional capacitance was about 5 pF, in good agreement with the value expected from the estimated cell surface, assuming a unit capacity of 1 $\mu\text{F}/\text{cm}^2$. The time constant of the capacity current was of the order of 100 μs , which shows that the series resistance due to the pipette tip is no more than 20 $\text{M}\Omega$. However, larger time constants were occasionally observed, indicating an incomplete disruption of the initial membrane patch.

Depolarizing voltage commands elicited Na and K currents which could be well resolved after compensation of the cell capacitance current (Fig. 16). The cell can be considered under excellent voltage clamp since, (i) at the peak inward current, the voltage drop across the series resistance is small (less than 2 mV in the experiment of Fig. 16, assuming a 20 $\text{M}\Omega$ series resistance), and (ii) the clamp settles within 100 μs as indicated above. The background noise was somewhat larger than that of a patch recording due to the conductance and capacitance of the cell. However, for small cells, resolution was still good enough to record large single channel responses. This is illustrated in Fig. 17 which shows individual ACh-activated channel currents in a chromaffin cell.

The pipette provides a low-resistance access to the cell interior which we used to measure intracellular potentials under current clamp conditions. The recordings showed spontaneous action potentials resembling those published by



Fig. 15 A and B. Capacitive current of a chromaffin cell. (A) After establishing a gigaseal on a chromaffin cell, a 20 mV pulse was applied to the pipette interior starting from a holding potential equal to the bath potential. The capacitance of the pipette and of the patch was almost completely compensated (see part I), resulting in very small capacitive artifacts. The pipette input resistance was 20 G Ω . (B) After disruption of the patch the response to a 3 mV pulse at a holding potential of -54 mV was measured. The capacitive current was much larger than in A, as the cell membrane capacitance had to be charged (compare the amplitudes of the voltage steps). From the integral of the capacitive current a cell membrane capacitance of 5 pF is calculated. The cell had a diameter of 13 μ m. Assuming a spherical shape, one obtains a unit capacitance of about 1 μ F/cm². The DC current was smaller than 2 pA, indicating a cell membrane resistance of several G Ω . The time constant of the capacitive current was less than 0.1 ms, which, together with the value of the cell capacitance, indicates a series resistance smaller than 20 M Ω .

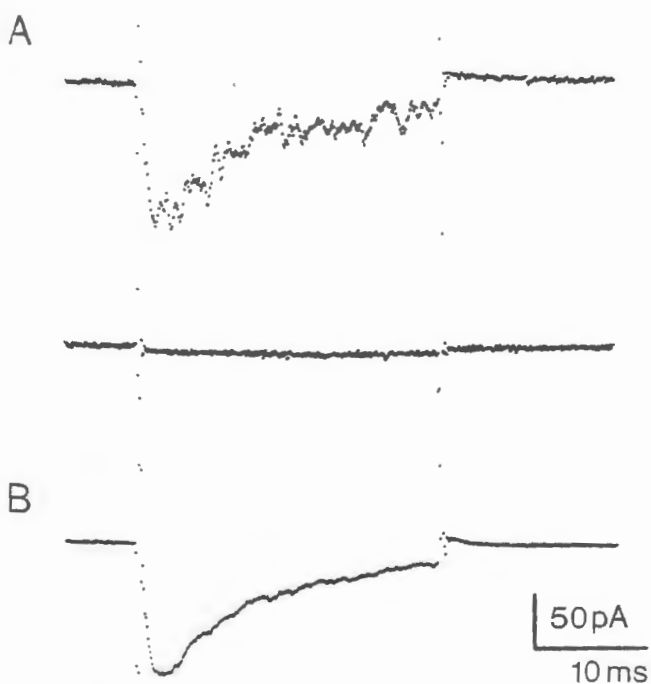


Fig. 16 A and B. Na currents in a chromaffin cell. (A) Single sweep responses to 34 mV depolarizing (above) and hyperpolarizing (below) pulses starting from a holding potential of -56 mV. (B) Average responses to 25 depolarizing voltage commands, as above. Room temperature; 1 kHz low pass

Brandt et al. (1976). The resting potential, averaging around -60 mV, displayed large fluctuations presumably due to spontaneous opening and closing of ionic channels. Similarly, action potentials and EPSPs could be recorded from small cultured spinal cord neurons.

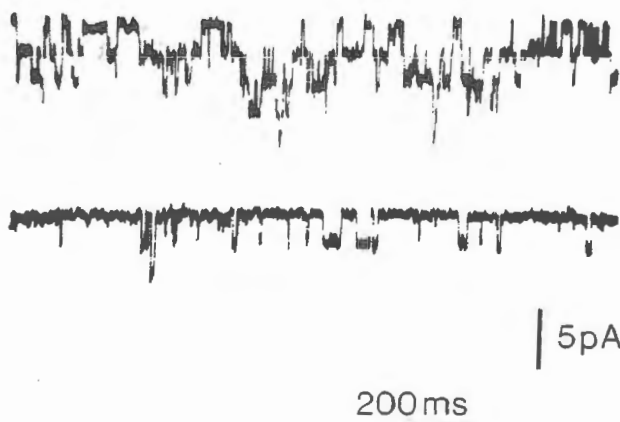


Fig. 17. Single channel records from a whole chromaffin cell. Normal bath solution with 100 μ M ACh added to the chamber. Single ACh-induced currents appeared at varying frequency due to slow changes in ACh concentration and due to desensitization. Two examples at different mean frequency are given. Holding potential was -65 mV; the amplitude of single channel currents was 2.3 pA and their mean open time approximately 30 ms. Filter bandwidth 200 Hz

When the pipette was withdrawn from the cell it sealed again, forming an outside-out patch (see Part III,2) of small dimensions. The pipette input capacitance dropped back to a value close to that observed during establishment of the initial giga-seal. Concomitantly background noise was reduced and small channel currents, like those of individual Na channels, could be observed.

In some experiments, the pipette was filled with a Cs-rich solution. The resting potential dropped from a normal value to zero within 10 s after disruption of the initial patch. This observation suggests that the intracellular solution exchanges quickly with the pipette interior. Thus, the method described in this section may be applied not only to record membrane currents, but also to alter the cell's ionic contents. Compared to the nystatin method (Cass and Dalmark 1973) it has the advantage to allow the exchange of divalent ions and of macromolecules.

The present method offers several advantages over the usual recording techniques using glass microelectrodes. It avoids the leakage due to cell penetration with the microelectrode, it allows reliable voltage clamp of small cells, and it offers the possibility of studying macroscopic currents and single channel currents in the same cell. It also allows at least partial control of the ionic milieu of the cell interior.

Conclusions

The methods described here provide several options for voltage- or current-clamp recording on cells or cell-free membrane patches. The size of the cells is not a restriction to the applicability of at least two of these methods. The only requirement is a freely accessible cell surface. This requirement is naturally fulfilled for a number of preparations. It is also fulfilled for most other preparations after enzymatic cleaning. The variety of cell types on which giga-seal formation has been successful is illustrated in Table 1.

The manipulations described here provide free access to either face of the membrane for control of the ionic environment. The giga-seal allows ionic gradients across the membrane to be maintained and high resolution measurements of current through the membrane to be performed.

Table 1. A listing of preparations on which giga-seals have been obtained. Only a fraction of the preparations have been investigated in detail. Bovine chromaffin cells and guinea pig liver cells were plated and kept in short term tissue culture. We acknowledge receiving cells from J. Bormann, T. Jovin, W. D. Krenz, E.-M. Neher, L. Piper, and G. Shaw, Göttingen, FRG; I. Schulz, Frankfurt, FRG; G. Trube, Homburg, FRG, and I. Spector, Bethesda, MD, USA

Cell lines in tissue culture:	Single cells:
Mouse neuroblastoma	Human and avian erythrocytes
Rat basophilic leukaemia cells	Mouse activated macrophages
Primary tissue culture:	Enzymatically dispersed cells:
Rat myotubes and myoballs	Bovine chromaffin cells
Mouse and rabbit spinal cord cells	Guinea pig heart myocytes
Rat cerebellar cells	Guinea pig liver cells
Rat dorsal root ganglion cells	Mouse pancreatic cells
Torpedo electrocytes	Enzyme treated cells:
Rat fibroblasts	Frog skeletal muscle fibres
	Rat skeletal muscle fibres
	Snail ganglion cells

The manipulations are simple and, with some practice, appear to be performed more easily than standard voltage clamp experiments. We expect that they will help to clarify physiological mechanisms in a number of preparations which, so far, have not been amenable to electrophysiological techniques.

Acknowledgements. We thank E. Fenwick for providing dispersed chromaffin cells. We also thank H. Karsten for culturing myoballs and Z. Vogel for a gift of Rhodamine-labelled α -bungarotoxin. O. P. Hamill and F. J. Sigworth were supported by grants from the Humboldt foundation. E. Neher and A. Marty were partially supported by the Deutsche Forschungsgemeinschaft.

References

- Brandt BL, Hagiwara S, Kidokoro Y, Miyazaki S. (1976) Action potentials in the rat chromaffin cell and effects of Acetylcholine. *J Physiol (Lond)* 263:417–439
- Cass A, Dalmark M (1973) Equilibrium dialysis of ions in nystatin-treated red cells. *Nature (New Biol)* 244:47–49
- Fenwick EM, Fajdiga PB, Howe NBS, Livett BG (1978) Functional and morphological characterization of isolated bovine adrenal medullary cells. *J Cell Biol* 76:12–30
- Gage PW, Van Helden D (1979) Effects of permeant monovalent cations on end-plate channels. *J Physiol (Lond)* 288:509–528
- Hamill OP, Sakmann B (1981) A cell-free method for recording single channel currents from biological membranes. *J Physiol (Lond)* 312:41–42P
- Horn R, Brodwick MS (1980) Acetylcholine-induced current in perfused rat myoballs. *J Gen Physiol* 75:297–321
- Horn R, Patlak JB (1980) Single channel currents from excised patches of muscle membrane. *Proc Natl Acad Sci USA* 77:6930–6934
- Kostyuk PG, Krishtal OA (1977) Separation of sodium and calcium currents in the somatic membrane of mollusc neurones. *J Physiol (Lond)* 270:545–568
- Kostyuk PG, Krishtal OA, Pidoplichko VI (1976) Effect of internal fluoride and phosphate on membrane currents during intracellular dialysis of nerve cells. *Nature* 257:691–693
- Krishtal OA, Pidoplichko VI (1975) Intracellular perfusion of *Helix* neurons. *Neurophysiol (Kiev)* 7:258–259
- Krishtal OA, Pidoplichko VI (1980) A receptor for protons in the nerve cell membrane. *Neuroscience* 5:2325–2327
- Läuger P (1975) Shot noise in ion channels. *Biochim Biophys Acta* 413:1–10
- Langmuir I (1938) Overturning and anchoring of monolayers. *Science* 87:493–500
- Lee KS, Akaie N, Brown AM (1978) Properties of internally perfused, voltage clamped, isolated nerve cell bodies. *J Gen Physiol* 71:489–508
- Neher E (1981) Unit conductance studies in biological membranes. In: Baker PF (ed), *Techniques in cellular physiology*. Elsevier/North-Holland, Amsterdam
- Neher E, Sakmann B (1976) Single channel currents recorded from membrane of denervated frog muscle fibres. *Nature* 260:799–802
- Neher E, Sakmann B, Steinbach JH (1978) The extracellular patch clamp: A method for resolving currents through individual open channels in biological membranes. *Pflügers Arch* 375:219–228
- Nir S, Bentz J (1978) On the forces between phospholipid bilayers. *J Colloid Interface Sci* 65:399–412
- Parsegian VA, Fuller N, Rand RP (1979) Measured work of deformation and repulsion of lecithin bilayers. *Proc Natl Acad Sci USA* 76:2750–2754
- Petrov JG, Kuhn H, Möbius D (1980) Three-Phase Contact Line Motion in the deposition of spread monolayers. *J Colloid Interface Sci* 73:66–75
- Sakmann B, Patlak J, Neher E (1980) Single acetylcholine-activated channels show burst-kinetics in presence of desensitizing concentrations of agonist. *Nature* 286:71–73
- Sigworth FJ, Neher E (1980) Single Na^+ channel currents observed in cultured rat muscle cells. *Nature* 287:447–449
- Stevens CF (1972) Inferences about membrane properties from electrical noise measurements. *Biophys J* 12:1028–1047

Received March 11 / Accepted May 27, 1981